

GEOMETRICAL INTERPRETATION OF THE ARC-LENGTH METHOD

M. FAFARD† and B. MASSICOTTE‡

†Department of Civil Engineering, Laval University, Québec City, Québec, G1K 7P4, Canada

‡Department of Civil Engineering, École Polytechnique de Montréal, Montréal, Québec,
 H3C 3A7, Canada

(Received 16 December 1991)

Abstract—The arc-length method is a powerful solution technique becoming increasingly popular among researchers and engineers. This method is presented here as a particular case of a more general formulation which includes all other solution strategies. The arc-length method is derived in its continuous and discrete formulations. Two versions of the arc-length method (Crisfield and Ramm) are presented and compared using a geometrical interpretation. Advantages and disadvantages of each method are pointed out. A new method, called the modified Crisfield–Ramm method, is proposed. This improved arc-length method combines the advantages of the two parent methods.

INTRODUCTION

The nature of special problems encountered in structural analysis often requires the use of sophisticated analytical techniques. Particularly, optimization constraints combined with safety requirements enhance the need for better understanding of structural behaviour. For these reasons, nonlinear finite element analysis of structures increases constantly. This type of analysis is used either as a powerful research tool, or in the design process of complex or unique structures. The objective of such an analysis is to obtain the equilibrium states of a structure at various load levels. All these equilibrium states trace the load–displacement response of the structure in which the applied load varies proportionally as a function of a unique load parameter. In such a case, for an n degree-of-freedom (DOF) system, $n + 1$ unknowns define completely the problem. The finite element method, based on continuum mechanics, provides n relationships describing the equilibrium states of a structure. This is expressed in a single equation

$$\{R(\{u\}, \lambda)\} = \lambda \{F\} - \{R_{\text{int}}(\{u\})\} = 0. \quad (1)$$

The parameters of this equation are $\{R(\{u\}, \lambda)\}$, the residual out-of-balance nodal forces; $\{u\}$, the n unknown DOF; λ , a scalar load parameter; $\{F\}$, the reference load vector; $\{R_{\text{int}}\}$, the internal nodal forces. To complete the definition of the problem with $n + 1$ unknowns, an additional equation is introduced, depending on the solution strategy adopted

$$f(\{u\}, \lambda) = 0. \quad (2)$$

The nonlinear response of a structure, related to geometrical and/or material nonlinearities, requires iterative solution techniques. At the current iteration

number i , the displacement field $\{u\}$ and the load parameter λ in the subsequent iteration, are given by

$$\{u^{i+1}\} = \{u^i\} + \{\Delta u^i\} \quad (3)$$

$$\lambda^{i+1} = \lambda^i + \Delta \lambda^i. \quad (4)$$

In these equations $\{\Delta u^i\}$ and $\Delta \lambda^i$ are the corrections of the displacement field and the load parameter, respectively. The iteration process, at a given load–displacement step, brings progressively eqns (1) and (2) toward zero, such that

$$\{R(\{u^{i+1}\}, \lambda^{i+1})\} \cong 0 \quad (5)$$

$$f(\{u^{i+1}\}, \lambda^{i+1}) \cong 0. \quad (6)$$

The evaluation of $\{\Delta u^i\}$ and $\Delta \lambda^i$ varies depending on the technique adopted. In most approaches, they are treated separately within each iteration.

The correction of the displacement field $\{\Delta u^i\}$ is calculated using various approaches. The most popular are the Newton–Raphson method, the BFGS technique [1], the nonlinear conjugated gradient method [2] or the preconditioned linear conjugated gradient method [3].

On the other hand, the correction of the load parameter $\Delta \lambda^i$ is based on techniques grouped in three families: load-controlled, displacement-controlled and arc-length methods. With load-controlled methods, λ^i is fixed at a certain level (thus $\Delta \lambda^i = 0$) and only $\{\Delta u^i\}$ varies in the iterative process. Oppositely, in displacement-controlled methods [4], $\Delta \lambda^i$ is calculated for a fixed increment of one displacement. In the various adaptations of the arc-length method [5–9], $\Delta \lambda^i$ varies as a function of the increment of all displacements. It can be seen as a generalized displacement-controlled method. As

shown later in this paper, these three families are particular cases of a more general formulation expressed in a single general equation.

This paper focuses on the constant arc-length method (CALM), particularly the Crisfield and Ramm adaptations. This method was found to be the most efficient one for the analysis of stable and unstable structures near limit points [3].

The objectives of the paper are as follows. It clarifies the various formulations of the arc-length method. Crisfield and Ramm's approaches are presented and compared, with advantages and disadvantages of each one clearly highlighted. A geometrical interpretation of the CALM is introduced. This new approach enhances the comprehension of the method and helps to develop a better feeling on the application of the CALM. Also, a new CALM, namely the modified Crisfield-Ramm method, is introduced. This method includes the best of the two parent methods, without their respective limitations. Finally, the paper concludes with examples illustrating the application of the CALM with the Crisfield, the Ramm and the Crisfield-Ramm methods.

THE ARC-LENGTH METHOD

The arc-length method is a solution strategy in which the path through a converged solution, at any step, follows a direction orthogonal to the tangent of the solution curve. In this procedure, both the load vector and the displacement field vary. The method is presented in the following sections in two forms. First, the arc-length method is introduced in its general, or continuous, formulation. This is followed by the presentation of the method in a discrete formulation, as implemented in computer programs.

General formulation

The equilibrium equation for a discrete structure is defined in eqn (1). The $n + 1$ independent variables of this equation are the n DOF u and the load parameter λ . These variables can be expressed as a function of the curvilinear coordinate system s along the load-displacement response of the structure (Fig. 1), such that $\{u\} = \{u(s)\}$ and $\lambda = \lambda(s)$. The tangent unit vector to curve s , t , is expressed as

$$\mathbf{t} = \begin{Bmatrix} \dot{u} \\ \dot{\lambda} \end{Bmatrix}, \quad (7)$$

where

$$\{\dot{u}\} = \frac{1}{m} \left\{ \frac{du}{ds} \right\}, \quad \dot{\lambda} = \frac{1}{m} \frac{d\lambda}{ds}.$$

The scaling factor of the vector is obtained by

$$m = \sqrt{\left\{ \frac{du}{ds} \right\}' \left\{ \frac{du}{ds} \right\} + \left(\frac{d\lambda}{ds} \right)^2}.$$

From eqn (7) one can write

$$\mathbf{t} \cdot \mathbf{t} = \{\dot{u}\}'\{\dot{u}\} + \dot{\lambda}^2 = 1. \quad (8)$$

As stated by [6], the first derivative of the equilibrium equation [eqn (1)] with respect to s is written as

$$\{\dot{R}\} = -[K_T] \left\{ \frac{\partial u}{\partial s} \right\} + \dot{\lambda} \left\{ \frac{\partial R}{\partial \lambda} \right\} = 0 \quad (9)$$

with

$$[K_T] = - \left[\frac{\partial R}{\partial u} \right].$$

Equation (9) can be simplified by using eqn (1) to define

$$\left\{ \frac{\partial R}{\partial \lambda} \right\} = \{F\}. \quad (10)$$

Thus, introducing eqn (10) in eqn (9) leads to

$$\{\dot{R}\} = -[K_T]\{\dot{u}\} + \dot{\lambda}\{F\} = 0 \quad (11)$$

which can be also expressed by

$$\{\dot{u}\} = \dot{\lambda}[K_T]^{-1}\{F\} \quad \{\dot{u}\} = \dot{\lambda}\{\Delta u_F\}$$

where

$$\{\Delta u_F\} = [K_T]^{-1}\{F\}. \quad (12)$$

Equation (12) allows redefining eqn (8) such that

$$\dot{\lambda}^2(1 + \{\Delta u_F\}'\{\Delta u_F\}) = 1. \quad (13)$$

Finally, using eqn (13), the tangent to the curve is defined by

$$(\{\dot{u}\}, \dot{\lambda}) = \frac{\pm 1}{\sqrt{\{\Delta u_F\}'\{\Delta u_F\} + 1}} (\{\Delta u_F\}, 1). \quad (14)$$

This formulation for $\{\dot{u}\}$ and $\dot{\lambda}$ represents the basic expression for the arc-length method. However, this form is not applicable in a finite element computer program, a discrete formulation of these relationships is thus introduced.

Discrete formulation

The relationships presented in the previous section can be expressed in a discrete formulation. The derivatives $\{\dot{u}\}$ and $\dot{\lambda}$ are given by

$$\{\dot{u}\} \cong \left\{ \frac{\Delta u}{\Delta S} \right\}, \quad \dot{\lambda} \cong \left\{ \frac{\Delta \lambda}{\Delta S} \right\}, \quad (15)$$

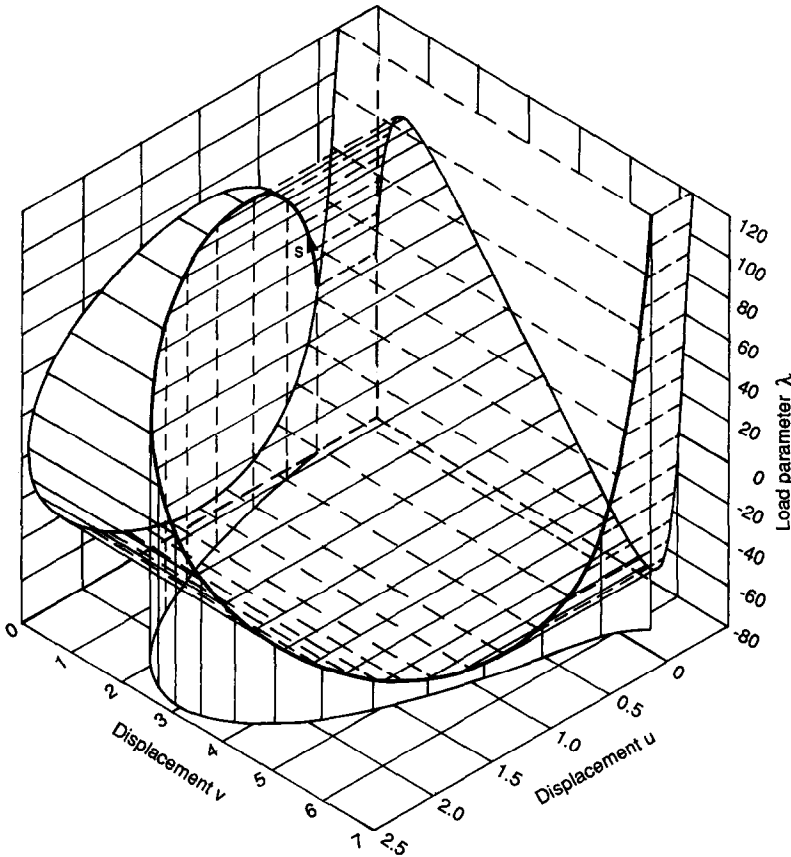


Fig. 1. Typical curve for a structure with two degrees-of-freedom.

where ΔS is a finite increment of the arc-length. Using the new definitions of eqn (15), the derivation of the equilibrium equation [eqn (11)] becomes

$$-[K_T]\{\Delta u\} + \Delta\lambda\{F\} = 0. \tag{16}$$

Using eqn (15), eqn (8) becomes

$$\{\Delta u\}^T\{\Delta u\} + (\Delta\lambda)^2 = (\Delta S)^2. \tag{17}$$

Solution techniques proposed by [5–8] are based on eqn (17). Equations (16) and (17) provide the $n + 1$ relationships required to solve nonlinear problems from the last converged step p to the next step $p + 1$

$$\{\Delta u^p\} = \Delta\lambda[K_T]^{-1}\{F\} = \Delta\lambda\{\Delta u_F\} \tag{18}$$

$$\Delta\lambda = \frac{\pm\Delta S}{\sqrt{\{\Delta u_F\}^T\{\Delta u_F\} + 1}} \tag{19}$$

$$\{u^{p+1}\} = \{u^p\} + \{\Delta u^p\} \tag{20}$$

$$\lambda^{p+1} = \lambda^p + \Delta\lambda^p. \tag{21}$$

For a given value of the arc-length increment ΔS , defined as the distance along the curve $(\{u\}, \lambda)$, it is possible to find the solution of the problem. However, since the correction expressed in eqns (20) and (21) is

linear, a small value for ΔS must be selected. Alternatively, an iterative method can be adopted to remain close to the actual curve $(\{u\}, \lambda)$.

THE CRISFIELD-RAMM ARC-LENGTH METHOD

Independently [7] and [8] proposed for eqn (2) the following relationship, based on eqn (17)

$$f(\{u\}, \lambda) = \{u_p^{p+1}\}^T\{u_p^{p+1}\} + (\lambda_p^{p+1})^2 - (\Delta S)^2 = 0. \tag{22}$$

Terms $\{u_p^{p+1}\}$ and λ_p^{p+1} in eqn (22) are the total increments in the displacement field and load factor respectively, from step p to step $p + 1$. These increments are obtained through an iterative process, expressed as

$$\{u_p^{p+1}\} = \{u^{p+1}\} - \{u^p\} = \sum_{\text{iterations}} \Delta u^i \tag{23}$$

$$\lambda_p^{p+1} = \lambda^{p+1} - \lambda^p = \sum_{\text{iterations}} \Delta\lambda^i. \tag{24}$$

In these equations, $(\{u^p\}, \lambda^p)$ is the last point of converged equilibrium on the response curve $(\{u\}, \lambda)$

whereas $(\{u^{p+1}\}, \lambda^{p+1})$ is the point of converged solution after an increment ΔS of the arc-length on the same curve. If ΔS remains constant from step p to $p + 1$, eqn (22) represents a hypersphere of radius ΔS in a $n + 1$ dimension space (Fig. 2).

GENERAL EXPRESSION

The various solution strategies commonly used in nonlinear analysis can be grouped in a single equation. The hypersphere expressed in eqn (22) was redefined by [3] in a more general expression in the $n + 1$ dimension space where $[P]$ is a diagonal matrix and d a scalar

$$f(\{u\}, \lambda) = \{u_p^{p+1}\}^T [P] \{u_p^{p+1}\} + d(\lambda_p^{p+1})^2 - \Delta S^2 = 0. \quad (25)$$

This equation includes the various methods used to solve nonlinear problems: load-controlled, displacement-controlled and arc-length methods. For a hypersphere, the terms P_{ij} of $[P]$ are equal to one only for $i = j$, and $d = 1$. For all $P_{ii} \neq 1$ and/or $d \neq 1$, eqn (25) becomes a hyperellipse. From eqn (25), one can extract the various expressions associated with other methods:

- the original Crisfield–Ramm arc-length method expressed in eqn (22) is obtained from eqn (25) when $[P] = [I]$ and $d = 1$;
- the load-controlled method corresponds to the case where all $P_{ij} = 0$ and $d = 1$ in eqn (25);
- the displacement-controlled method is obtained when $d = 0$ and only one $P_{ij} = P_{kk} \neq 0$, corresponding to the prescribed displacement u_k ;
- with the arc-length method, matrix $[P]$ can be set up to consider only certain degrees-of-freedom and eliminate other ones (e.g. $P_{ii} = 1$ for translations and $P_{ii} = 0$ for rotations).

Both [7] and [8] proposed similar simplifications to eqn (25) where $[P] = [I]$ and $d = 0$. In its approach,

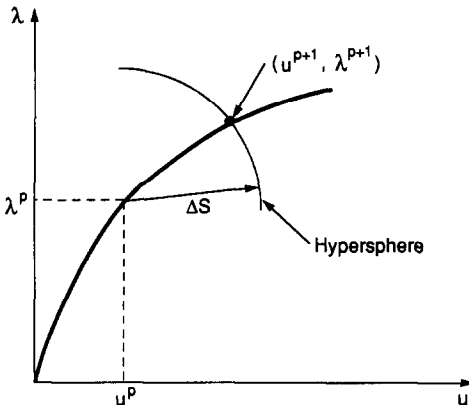


Fig. 2. Example of a hypersphere (circle) for a one degree-of-freedom system.

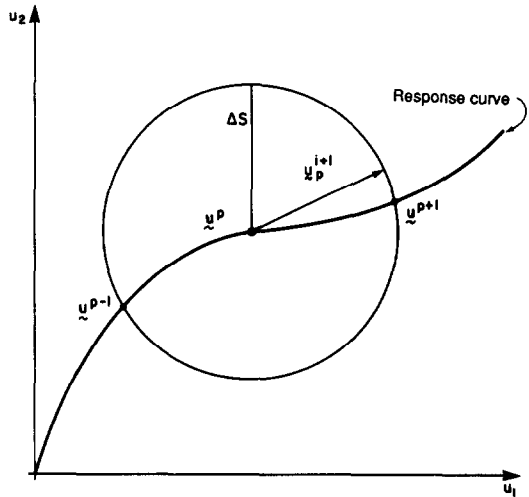


Fig. 3. Crisfield’s method for a two degree-of-freedom system.

Crisfield forces the length of the displacement increment to remain equal to the arc-length at each iteration from step p to step $p + 1$

$$\{u_p^i\}^T \{u_p^i\} = \{u_p^{p+1}\}^T \{u_p^{p+1}\} = \Delta S^2. \quad (26)$$

It is thus a constant arc-length approach. Ramm, on the other hand, limits only the length of the displacement increment for the first iteration ($i = 1$)

$$\{\Delta u^1\}^T \{\Delta u^1\} = \Delta S^2 \quad (27)$$

and, as discussed later in this paper, proposes another technique for the subsequent iterations. In this case, the arc-length in subsequent iterations varies from the initial ΔS .

Equations (26) and (27) describe a hypersphere in the n degree-of-freedom space (Fig. 3). Crisfield and Ramm methods are described and compared in more details in the following sections.

CRISFIELD METHOD

With Crisfield’s method, $\{u_p^{p+1}\}$ can be rewritten for iteration i between steps p and $p + 1$

$$\{u_p^{i+1}\} = \{u^i\} - \{u^p\} + \{\Delta u^i\}. \quad (28)$$

With the decomposition of $\{\Delta u^i\}$ in two parts as proposed by [4], $\{u_p^{i+1}\}$ is expressed as

$$\{u_p^{i+1}\} = \{u^i\} - \{u^p\} + \{\Delta u_R^i\} + \Delta \lambda^i \{\Delta u_F^i\}, \quad (29)$$

where

$$\{\Delta u_R^i\} = [K_T^i]^{-1} \{R^i\} \quad (30)$$

$$\{\Delta u_F^i\} = [K_T^i]^{-1} \{F^i\}. \quad (31)$$

With Crisfield's approach, eqn (26) is rewritten using eqns (28)–(31) in a second-order form

$$a(\Delta\lambda^i)^2 + 2b(\Delta\lambda^i) + c = 0 \quad (32)$$

with

$$a = \{\Delta u_F^i\}^t \{\Delta u_F^i\}$$

$$b = \{\Delta u_F^i\}^t \{v^i\}$$

$$c = \{v^i\}^t \{v^i\} - \Delta S^2$$

$$\{v^i\} = \{\Delta u_R^i\} + \{u_p^i\}.$$

Equation (32) is applied at each iteration forcing displacements $\{u_p^{i+1}\}$ to be equal to ΔS from steps p to $p + 1$ so that $\|u_p^1\| = \dots = \|u_p^{i-1}\| = \|u_p^i\| = \|u_p^{i+1}\| = \dots = \|u_p^{p+1}\|$, where $\|\cdot\|$ denotes the Euclidian norm.

Geometrical interpretation

Geometrical interpretation of Crisfield's arc-length method is done in the n dimension space. Figure 3 illustrates the geometrical interpretation of eqn (32) in a two degree-of-freedom system. With $\{u^p\}$ last known point (converged solution) along the curve, eqn (32) traces a circle (hypersphere) of radius ΔS centred at $\{u^p\}$. For a sufficiently regular response and prior to any complete material failure, eqn (32) intersects the curve at two points. All displacement vectors $\{u^i\}$ touch the circle (hypersphere) at each iteration since vector $\{u_p^{i+1}\}$ keeps the same length ΔS .

Choice of the appropriate root

Since there are two roots for eqn (32), a criterion to select the appropriate root based on the least positive cosine value for the angle between $\{u_p^i\}$ and $\{u_p^{i+1}\}$ (for $i > 1$) is proposed [7]

$$\cos \theta^i = \frac{\{u_p^i\}^t \{u_p^{i+1}\}}{\|\{u_p^i\}\| \|\{u_p^{i+1}\}\|}. \quad (33)$$

This criterion is founded on the assumption that the appropriate solution vector $\{u_p^{i+1}\}$ should have about the same orientation as vector $\{u_p^i\}$. Thus only the root $\Delta\lambda^i$ leading to the least cosine is retained. This is illustrated in Fig. 4 where the good solution is obtained with the first root. At the first step ($p = 0$; $i = 1$), since $\{\Delta u_R\}$ is zero, eqn (32) becomes

$$\Delta\lambda^1 = \frac{\Delta S}{\sqrt{\{\Delta u_F\}^t \{\Delta u_F\}}}. \quad (34)$$

With eqn (34), the initial arc-length is evaluated by imposing at the first step, a load increment $\Delta\bar{\lambda}$

$$\Delta S = \Delta\bar{\lambda} \sqrt{\{\Delta u_F\}^t \{\Delta u_F\}}.$$

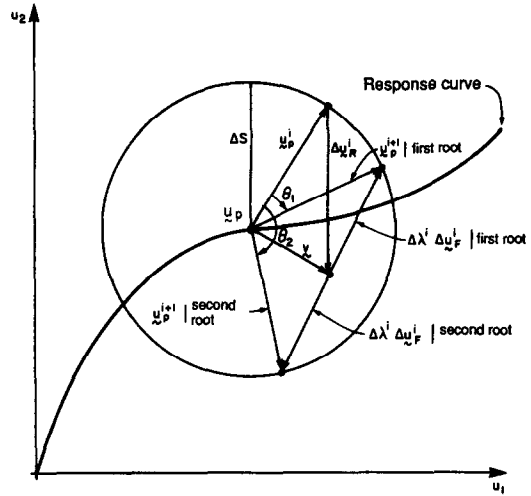


Fig. 4. Selection of the good root for eqn (32) for a two degree-of-freedom system.

At the beginning of step $p + 1$ ($i = 1$), the first load vector increment is evaluated as

$$\Delta\lambda^1 = \frac{\Delta S}{\sqrt{\{\Delta u_F\}^t \{\Delta u_F\}}} (\text{sign of } A) \quad (35)$$

with

$$A = \{u_{p-1}^p\}^t \{\Delta u_F\}.$$

Equation (35) is similar to eqn (19) without the term 1 under the square root since Crisfield's method operates in the n dimension space whereas eqn (19) is defined in the $n + 1$ dimension space. Strictly speaking, Crisfield's (or Ramm's) method should be called a 'pseudo' arc-length method although it is frequently referred to as the arc-length method.

The criterion expressed by eqn (35) is illustrated in Fig. 5 in the case where the arc-length ΔS at steps p and $p + 1$ are taken equal. For a smooth response, the hypersphere touches the curve at two points and eqn (35) defines the tangent to the curve at point p . The appropriate sign in eqn (35) produces a positive projection of $\Delta\lambda^1 \{\Delta u_F\}$ on $\{u_p^{i+1}\}$ to avoid a solution toward the previous converged point $p - 1$. Since ΔS and the square root term in eqn (35) are positive quantities, the sign of A is positive along loading branches of the response curve and is negative along unloading portions of the curve.

Guarantee of convergence

At this stage, the existence of at least one real root for eqn (32) must be established. This is done using the geometrical interpretation presented before. The requirement to have at least one real root for eqn (32) is a positive value for the square root term ($b^2 - ac \geq 0$). This is written as

$$(\{\Delta u_F\}^t \{v^i\})^2 \geq \|\{u_F^i\}\|^2 (\|\{v^i\}\|^2 - \Delta S^2). \quad (36)$$

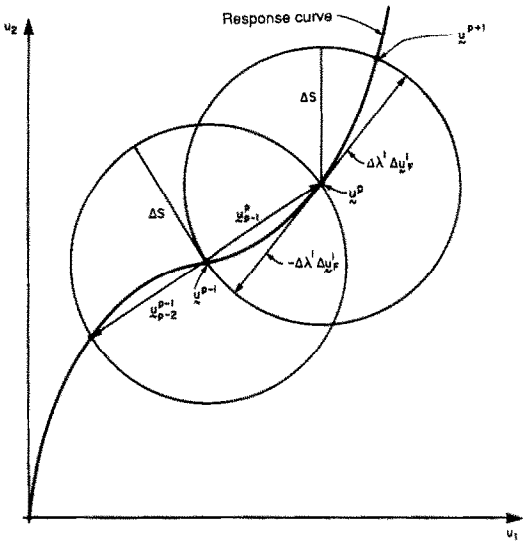


Fig. 5. Selection of the sign of $\Delta\lambda^1$ at the beginning of step $p + 1$ for a two degree-of-freedom system.

If β^i is the angle between $\{\Delta u_F^i\}$ and $\{v^i\}$, the term in parentheses in the left-hand side of eqn (36) is expressed by

$$\{\Delta u_F^i\}^t \{v^i\} = \|\{\Delta u_F^i\}\| \|\{v^i\}\| \cos \beta^i. \quad (37)$$

By introducing eqn (37) into eqn (36), one obtains

$$(\cos \beta^i)^2 \geq 1 - \frac{\Delta S^2}{\|\{v^i\}\|^2}. \quad (38)$$

The most restrictive case corresponds to $\cos \beta^i = 0$, obtained when $\{\Delta u_F^i\}$ and $\{v^i\}$ are orthogonal to each other. The condition for a positive square root term is then

$$\|\{u_p^i\} + \{\Delta u_R^i\}\| = \|\{v^i\}\| \leq \Delta S. \quad (39)$$

Figure 6 illustrates this condition for a two degree-of-freedom problem. It simply stipulates real roots always exist when $\{v^i\}$ stays within the hypersphere of radius ΔS . For $\{v^i\}$ precisely on the hypersphere, one obtains

$$\Delta\lambda^i = 0, \text{ for } \{v^i\}^t \{\Delta u_F^i\} = 0$$

$$\Delta\lambda_1^i = -\frac{2\{\Delta u_F^i\}^t \{v^i\}}{\{u_F^i\}^t \{\Delta u_F^i\}} \text{ and } \Delta\lambda_2^i = 0,$$

for

$$\{v^i\}^t \{\Delta u_F^i\} \neq 0. \quad (40)$$

However, when $\{v^i\}$ (or $\{\Delta u_R^i\}$) is outside the hypersphere, one cannot guarantee a real root. For a given $\{\Delta u_F^i\}$ there is however a zone where $\{\Delta u_R^i\}$ must be found to have a solution.

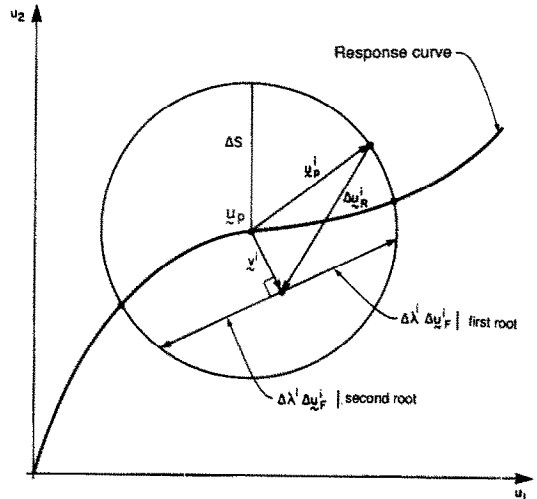


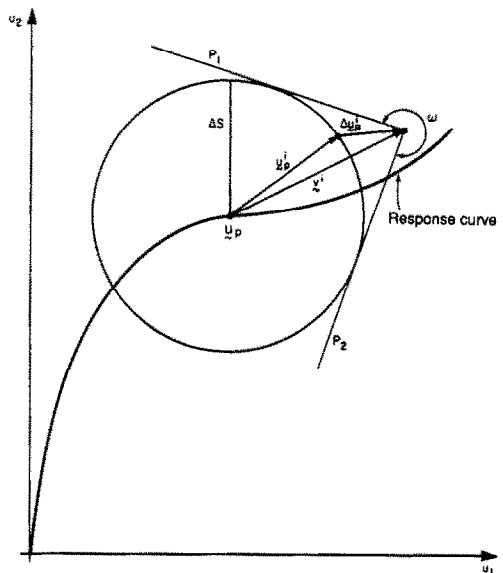
Fig. 6. Two real roots for a two degree-of-freedom system.

Figure 7 shows a fictitious example for a two degree-of-freedom problem in which $\{\Delta u_R^i\}$ (or $\{v^i\}$) falls outside the hypersphere. In this example, $\{\Delta u_F^i\}$ must be located within P_1 and P_2 lines (or two hyperplanes) to reach the hypersphere from the outside and thus produce a real root $\Delta\lambda^i$.

Finally, it should be mentioned that the demonstration presented above also applies to eqn (25). Conclusions drawn before remain true in the case where $d \neq 0$, leading to a hyperellipse in the $n + 1$ dimension space. To apply the Crisfield's arc-length method, an algorithm is given in Fig. 8.

RAMM ARC-LENGTH METHOD

As mentioned before, Ramm [8] proposed a method, similar to the Crisfield's one, called the



ω is the angle between v^i and Δu_F^i delimiting the zone where they do not exist real roots.

Fig. 7. Two imaginary roots for a two degree-of-freedom system.

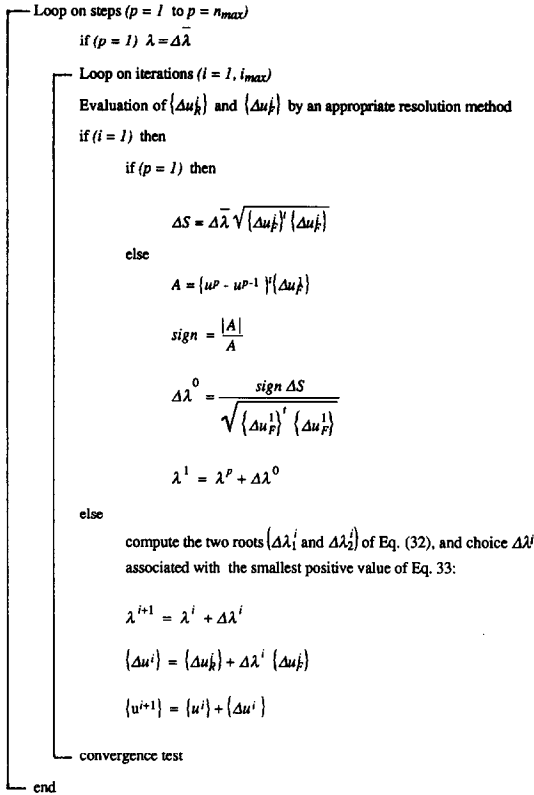


Fig. 8. Flow chart of Crisfield's arc-length method.

modified Riks-Wempner method. He proposed two approaches, in the $n + 1$ or in the n dimension space. The discussion presented hereafter is limited to the second case only.

As stated by eqn (27), only the first displacement increment $\{u_p^1\}$ must fall on the hypersphere of radius ΔS . With the modified Riks-Wempner method proposed by Ramm, the solution along the curve is found by following a line (or hyperplane) orthogonal to $\{u_p\}$ ($\equiv \{\Delta u^1\}$) expressed by

$$\{\Delta u^1\}^t \{\Delta u^i\} = 0. \tag{41}$$

Using the separation of $\{\Delta u^i\}$ in two parts ($\{\Delta u_k^i\}$ and $\{\Delta u_F^i\}$), as given by eqns (29)–(31), the load factor increment becomes

$$\Delta \lambda^i = - \frac{\{\Delta u^1\}^t \{\Delta u_k^i\}}{\{\Delta u^1\}^t \{\Delta u_F^i\}}. \tag{42}$$

Ramm's arc-length method is illustrated in Fig. 9 for a fictitious two degree-of-freedom system. By opposition to Crisfield's method, the solution with Ramm's method does not fall on the initial hypersphere. Due to eqn (41), the increment of displacement vector $\{\Delta u^i\}$ leaves the initial hypersphere at the second iteration. Therefore the arc-length ΔS varies at each iteration. One advantage of the Ramm's method is that there is only one value for $\Delta \lambda^i$, given by the linear eqn (42). Convergence is always possible

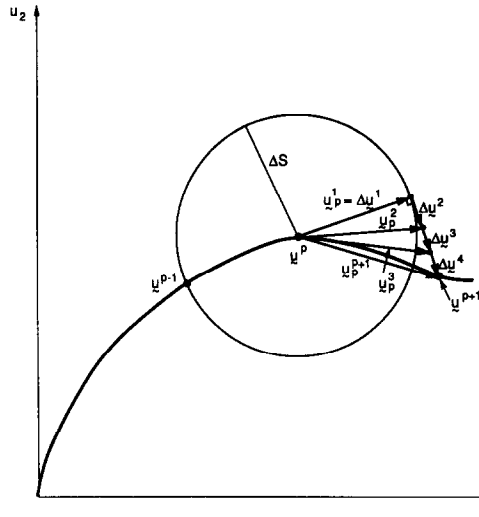


Fig. 9. Ramm's method for a two degree-of-freedom system.

as long as it exists physically. Beyond material failure points, ΔS increases rapidly, indicating the complete failure of the structure modelled. However, near limit points, a too large value for ΔS may lead to a solution much too far on the solution curve, as illustrated in Fig. 10. This can be avoided by using a smaller arc-length in order to follow more closely the solution curve.

To help implementing Ramm's arc-length method in computer programs, a flow chart is presented in Fig. 11.

MODIFIED CRISFIELD-RAMM ARC-LENGTH METHOD

Advantages and disadvantages of the original methods

Crisfield's and Ramm's methods offer many advantages but are both limited in their applicability due to some disadvantages.

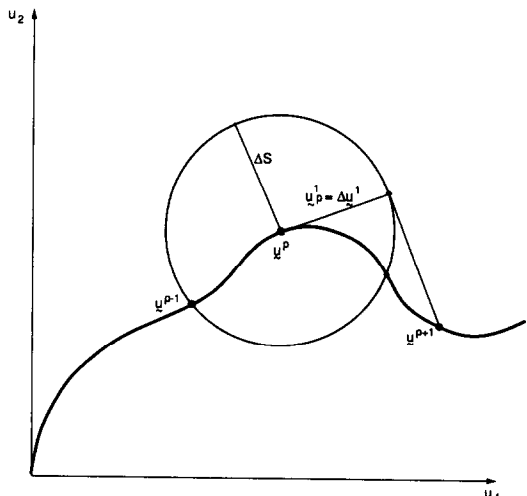


Fig. 10. Convergence problem for the Ramm's method for a two degree-of-freedom system.

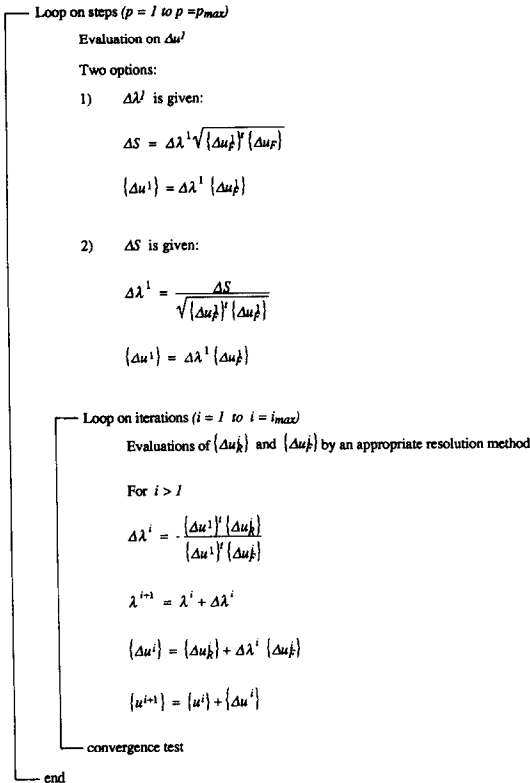


Fig. 11. Flow chart of Ramm's arc-length method.

Crisfield's arc-length method has the advantage of limiting the length of the displacement increment, for all iterations within a step, to a constant value ΔS . This avoids non-convergence problems, particularly when the stiffness of a system changes rapidly due to occurrence of plasticity or due to cracking in brittle structures. However, this method may lead to complex roots when solving eqn (32). This was observed by [3] in some situations. Also, eqns (33) and (35), used to select the good real root to avoid a solution

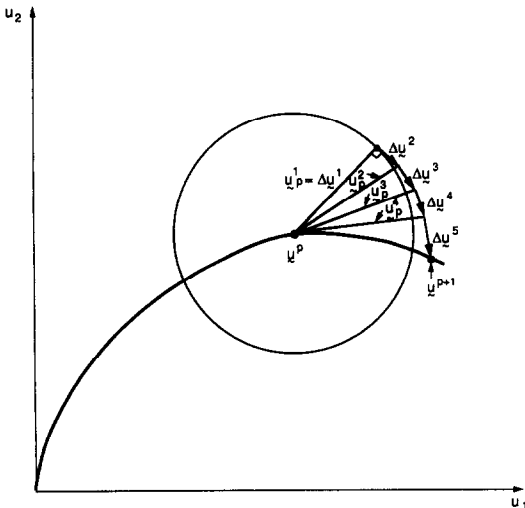
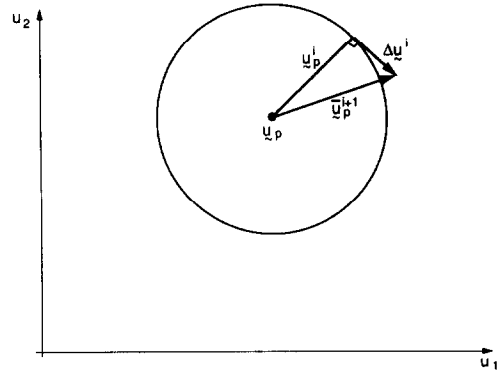
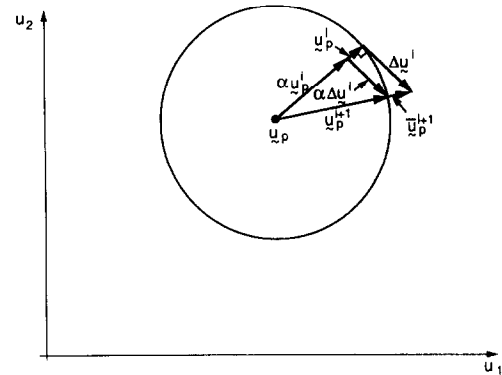


Fig. 12. Updated hyperplane Ramm's method for a two degree-of-freedom system.



a) Original Ramm's arc-length method.



b) Modified Crisfield-Ramm's arc-length method.

Fig. 13. Proposed modified Crisfield-Ramm's method.

towards the previous converged solution, do not guarantee a correct choice.

Ramm's arc-length method offers the advantage of simplicity, and guarantees the solution. Also, in most cases, this method gives the same results as with Crisfield's approach. However, the arc-length ΔS is imposed only at the first iteration. This can lead, in rare occasions where there is an abrupt change in the response, to difficulties in tracing the load-displacement response of a structure.

Nevertheless, Ramm's method has more advantages than the Crisfield's approach, although the difference is minute. It is, however, possible to combine the two methods to take advantage of the good points of both approaches.

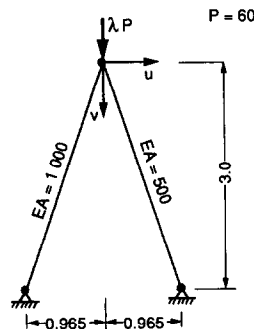


Fig. 14. Two degree-of-freedom structure of the example.

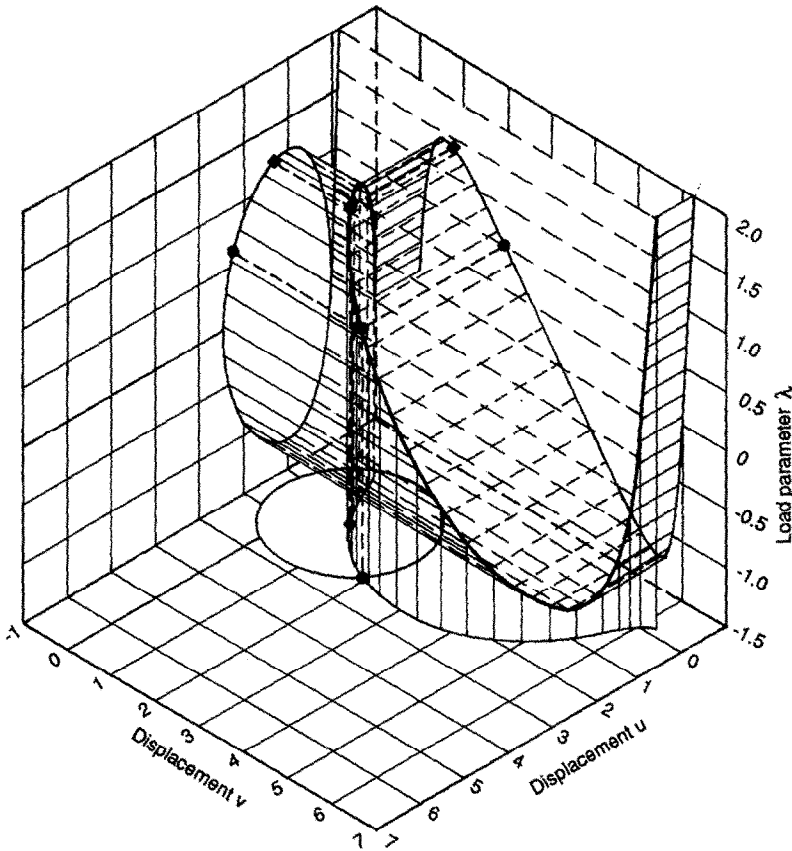


Fig. 15. Load-displacements curve of the structure in Fig. 12.

The proposed approach

A new method called the modified Crisfield-Ramm arc-length method (MCR) is proposed hereafter. This

method is based on the constraint equation proposed by Ramm and expressed now as

$$\{\Delta u_p^i\}^T \{\Delta u^i\} = 0. \tag{43}$$

Table 1. Crisfield's arc-length method ($\Delta S = 1.502$)

Iteration No. <i>i</i>	Δu_F^i	Δu_R^i	$\Delta \lambda^i$	Δu^i	u^i	λ^i
1	$\langle 4.434$ $-3.394 \rangle$	$\langle 0 \ 0 \rangle$	-0.2691	$\langle 1.193$ $0.9135 \rangle$	$\langle 2.502$ $1.652 \rangle$	0.9328
2	$\langle 0.9035$ $2.171 \rangle$	$\langle 7.023 \times 10^{-2}$ $0.6314 \rangle$	-0.1794	$\langle -0.2323$ $0.2419 \rangle$	$\langle 2.270$ $1.894 \rangle$	0.7534
3	$\langle -0.9569$ $-2.325 \rangle$	$\langle -0.1651$ $-0.2709 \rangle$	-0.1304	$\langle -4.035 \times 10^{-2}$ $-3.240 \times 10^{-2} \rangle$	$\langle 2.229$ $1.926 \rangle$	0.6230
4	$\langle -0.7380$ $-1.783 \rangle$	$\langle -2.686 \times 10^{-3}$ $-3.173 \times 10^{-3} \rangle$	-2.231×10^{-3}	$\langle -1.039 \times 10^{-3}$ $8.048 \times 10^{-4} \rangle$	$\langle 2.228$ $1.927 \rangle$	0.6208

Table 2. Ramm's arc-length method ($\Delta S = 1.502$)

Iteration No. <i>i</i>	Δu_F^i	Δu_R^i	$\Delta \lambda^i$	Δu^i	u^i	λ^i	ΔS
1	$\langle 4.434$ $-3.394 \rangle$	$\langle 0 \ 0 \rangle$	-0.2691	$\langle 1.193$ $0.9135 \rangle$	$\langle 2.502$ $1.652 \rangle$	0.9328	1.502
2	$\langle 0.9035$ $2.171 \rangle$	$\langle -7.023 \times 10^{-2}$ $0.6314 \rangle$	-0.1610	$\langle -0.2157$ $0.2818 \rangle$	$\langle 2.286$ $1.934 \rangle$	0.7718	1.544
3	$\langle -0.9106$ $-2.309 \rangle$	$\langle -0.1967$ $-0.3620 \rangle$	-0.1772	$\langle -3.534 \times 10^{-2}$ $4.616 \times 10^{-2} \rangle$	$\langle 2.251$ $1.980 \rangle$	0.5946	1.558
4	$\langle -0.6925$ $-1.775 \rangle$	$\langle -3.937 \times 10^{-3}$ $-6.531 \times 10^{-3} \rangle$	-4.356×10^{-3}	$\langle -9.205 \times 10^{-4}$ $1.201 \times 10^{-3} \rangle$	$\langle 2.250$ $1.981 \rangle$	0.5902	1.559

This equation uses the updated hyperplane $\{\Delta u^i\}$, and eqn (42) is now rewritten as

$$\Delta \lambda^i = - \frac{\{u_p^i\}' \{\Delta u_R^i\}}{\{u_p^i\}' \{\Delta u_F^i\}}. \tag{44}$$

Figure 12 illustrates this modified method for a two-dimensional problem. One observes that the arc-length ΔS increases compared to the value at the first iteration. At iteration i , the current displacement is obtained by

$$\{\tilde{u}_p^{i+1}\} = \{u_p^i\} + \{\Delta u^i\}. \tag{45}$$

However, as shown in Fig. 13(a), $\{\tilde{u}_p^{i+1}\}$ does not fall on the circle (hypersphere) defined initially. To bring $\{\tilde{u}_p^{i+1}\}$ back on the initial hypersphere, it is necessary to reduce the magnitude $\{\tilde{u}_p^{i+1}\}$ such that

$$\|u_p^{i+1}\| = \Delta S = \alpha \|\tilde{u}_p^{i+1}\| \tag{46}$$

which gives

$$\alpha = \frac{\Delta S}{\|\tilde{u}_p^{i+1}\|}. \tag{47}$$

Equations (45)–(47) allow to express the desired incremental displacement

$$\{u_p^{i+1}\} = \alpha \{u_p^i\} + \alpha \{\Delta u^i\}. \tag{48}$$

Figure 13 illustrates the effect of the constraint, from the application of eqn (45) in Fig. 13(a) to the effect of eqn (48) in Fig. 13(b). With the MCR method, the orthogonality between the updated hypersphere and $\{\Delta u^i\}$ and arc-length ΔS are preserved.

This new method does not induce any convergence problem and the response of structures is more easy to follow near limit points. Like in the other arc-length methods, near limit point and failure, some convergence problem can occur. This can be solved by reducing the ΔS value.

APPLICATION OF THE ARC-LENGTH METHOD

The two arc-length methods presented in this paper are, in the authors' opinion, the most reliable ones. Their implementation is easy and users become familiar quickly in the analysis of structures with the arc-length method. The reason for such performance is due to the great flexibility of the method in which the predominant degrees-of-freedom are recognized by the method and, therefore, govern the response.

A second important aspect with both Crisfield's and Ramm's approaches is that they involve only degrees-of-freedom [eqns (26), (27), (34), (35), (41) and (42)], whereas in some other arc-length methods load terms and degrees-of-freedom are mixed up [eqns (13) and (14)]. Although mathematically (or vectorially) there is no problem applying such

Table 3. Modified Crisfield-Ramm's method ($\Delta S = 1.502$)

Iteration No. i	Δu_i^i	Δu_k^i	$\Delta \lambda^i$	Δu^i	\tilde{u}_p^{i+1}	α	u_p^{i+1}	u^i	λ^i	ΔS
1	$\langle 4.434$ $-3.394 \rangle$	$\langle 0 \ 0 \rangle$	-0.2691	$\langle 1.193$ $0.9135 \rangle$	$\langle 1.193$ $0.9135 \rangle$	1	$\langle 1.193$ $0.9135 \rangle$	$\langle 2.502$ $1.652 \rangle$	0.9328	1.502
2	$\langle 0.9035$ $2.171 \rangle$	$\langle -7.023 \times 10^{-2}$ $0.6314 \rangle$	-0.1610	$\langle -0.2157$ $0.2818 \rangle$	$\langle 0.9732$ $1.195 \rangle$	0.9732	$\langle 0.9514$ $1.163 \rangle$	$\langle 2.260$ $1.9019 \rangle$	0.7718	1.502
3	$\langle -0.8926$ $-2.166 \rangle$	$\langle -0.1648$ $-0.2995 \rangle$	-0.1499	$\langle -3.099 \times 10^{-2}$ $2.535 \times 10^{-3} \rangle$	$\langle 0.9204$ $1.189 \rangle$	0.9996	$\langle 0.9201$ $1.188 \rangle$	$\langle 7.229$ $1.927 \rangle$	0.6218	1.502
4	$\langle -0.7359$ $-1.778 \rangle$	$\langle -1.280 \times 10^{-3}$ $-1.514 \times 10^{-3} \rangle$	-1.071×10^{-3}	$\langle -1.071 \times 10^{-3}$ $5.018 \times 10^{-4} \rangle$	$\langle 0.9196$ $1.188 \rangle$	1.0	$\langle 0.9196$ $1.188 \rangle$	$\langle 2.228$ $1.927 \rangle$	0.6208	1.502

methods, this can cause many inconveniences in numerical solutions [3] since the nature of the various terms involved differs.

In continuum mechanics, vector $\{u\}$ contains only displacements. However, in analysis of thin structures using plate or shell element or in structural analysis with beam elements, rotation terms are found among the degrees-of-freedom. A diagonal matrix $[P]$ with terms $P_{ii} = 0$ for rotations can be used to eliminate rotational degrees-of-freedom in order to add and multiply terms having the same nature. However, products of rotations (in radians), as they appear in the relationships pertaining to the arc-length method, are usually negligible compared to products of displacements.

The application of the arc-length method, as proposed in this paper, has been used very successfully in various types of analysis. Nonlinear response of a thin web open section under axial load and bending moments was studied by [10] using Crisfield's method where both geometrical and material nonlinearities were considered. Also, [3] applied the same technique in the stability analysis of plates and shells. Both used the finite element code MEF (standing for 'Méthode des Éléments Finis') available at Laval University. On the other hand, Ramm's method implemented in the finite element code NISA [11] developed at Stuttgart in Germany, was used by [12] for the postbuckling analysis of large diameter thin steel cylinders subjected to shear forces. It also was used by [13]

and [14] in the analysis of concrete panels and of thin reinforced concrete plates supported along their four edges and subjected simultaneously to inplane loads and transverse loads. In these last two cases, geometrical and material nonlinearities were involved.

The availability of the two methods in the same nonlinear finite element program is a good asset. They can be used for different applications but it is also possible to switch from one method to the other whenever required. Crisfield's method would be better suited when the arc-length ΔS increases too rapidly with Ramm's method. On the other hand, Ramm's approach can be used when Crisfield's method fails to obtain a real root. The MCR method, combining the advantages of the two parent methods, is believed to be the ideal one.

EXAMPLE

An example is presented to illustrate the arc-length method proposed by Crisfield and to compare it to Ramm's method and the MCR's method. The structure studied is made of two bar elements with different axial stiffnesses (Fig. 14). Small elastic strain assumption is assumed, the second Piola-Kirchhoff stress tensor is used whereas the Green-Lagrange strain tensor is adopted. Moreover, only the overall stability is considered and no individual buckling of bars is allowed. All these restrictions are not necessary but are imposed to simplify the interpretation of

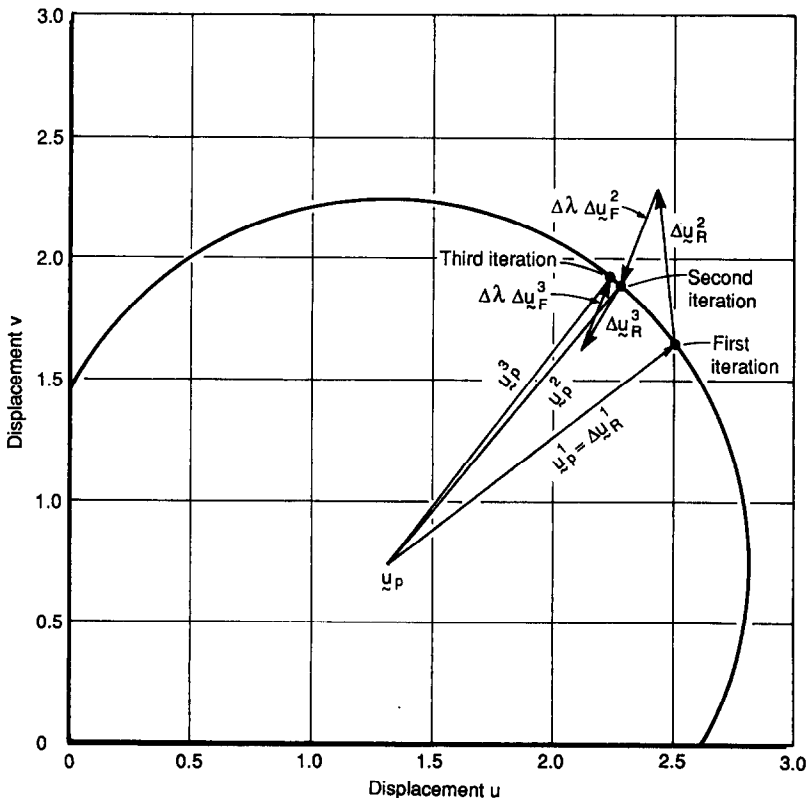


Fig. 16. First three iterations with the Crisfield's method.

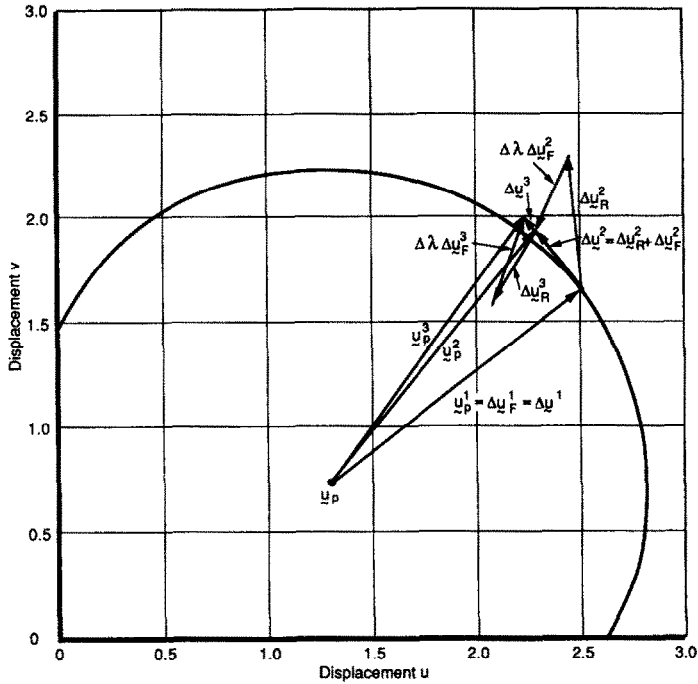


Fig. 17. First three iterations with the Ramm's method.

the results. This two degree-of-freedom example was selected so that one can visualize the geometrical variation of u and v simultaneously with the load factor λ .

Figure 15 illustrates the structure response in the $\lambda-u-v$ space where its projections on each plane are shown. On the $\lambda-v$ plane, one recognizes the typical limit point instability curve. The beginning of the

analysis with both Ramm's and Crisfield's methods is identified by a diamond shaped sign on each curve in Fig. 15. On the $u-v$ plane, the circle with a radius ΔS equal to 1.502, intersects the solution curve using Crisfield's method. Since Ramm's method is different, the solution slightly differs. The coordinates of the starting point are: $\lambda_1 = 1.202$, $u_1 = 1.31$ and $v_1 = 0.74$.

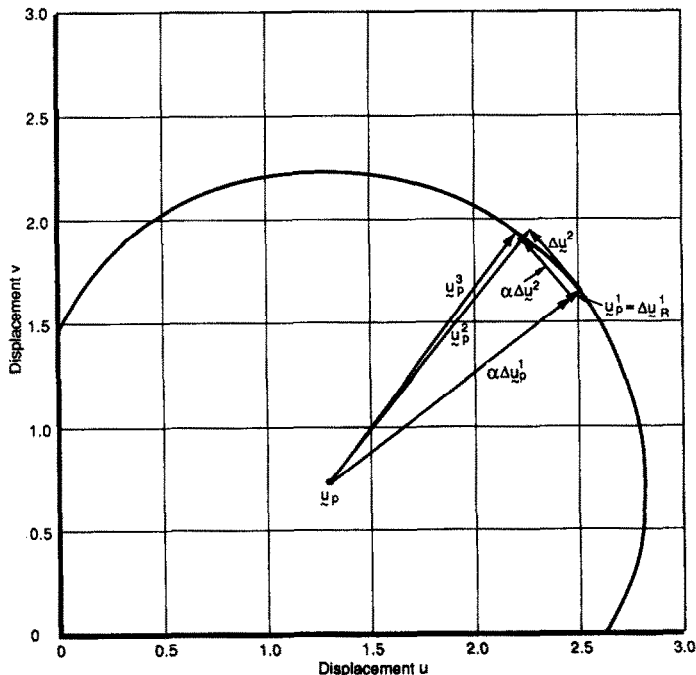


Fig. 18. First three iterations with the modified Crisfield-Ramm's method.

Tables 1–3 summarize the most important results obtained with the three approaches up to the fourth iteration. Figure 16 illustrates the path obtained with Crisfield's method for the first three iterations. At the second iteration vector $\{v^i\} = \{u_p^i\} + \{\Delta u_R^i\}$ is pointing outward the circle whereas at the third iteration, the same vector is pointing inward the circle. This fact illustrates that vector $\{v^i\}$ points inward the circle (or sphere) near convergence.

Results in Table 2 and Fig. 17 show that the arc-length ΔS with Ramm's method increases at each iteration. We observe also that $\{\Delta u^2\}$ and $\{\Delta u^3\}$ are orthogonal to $\{\Delta u^1\}$. Although the difference between Ramm's and Crisfield's approaches is small in the example, it can be larger for other problems. In this particular case the small difference is due to the flatness of the curve within a circle of small radius.

Figure 18 illustrates the same example for the MCR method. The comparison begins at the same point as in the two previous methods. After the first iteration, the same displacement $\{u^i\}$ (Table 3) is obtained. In the second iteration, $\Delta \lambda$ is computed as the Ramm's method. With the MCR method, the α parameter is calculated to respect the arc-length method. This is illustrated for the second iteration, in Fig. 18. Results in Table 3 show that this method converges exactly to the same displacements $\{u\}$ as the Crisfield's method.

CONCLUSION

In this paper, the arc-length method for the resolution of nonlinear response of various types of structures was presented. The attention was focused on the Crisfield's and Ramm's methods which were found to be the most efficient ones for the analysis of structures near limit points. A new geometrical interpretation of the method was presented and, based on this interpretation, a criterion proving the existence of a real root for Crisfield's approach was introduced. The authors presented a modified Crisfield–Ramm's method combining the advantages of the two previous methods. The example presented in the paper illustrated the similarity of the three methods and their ability to lead rapidly to a converged solution.

Finally, the authors believe that the modified method and the two other methods should be included in any nonlinear finite element program, since they can be used for different applications. Moreover, in many cases, the arc-length method replaces advan-

tageously the load-controlled or the displacement-controlled method.

Acknowledgement—The authors gratefully thank the National Sciences and Engineering Research Council of Canada for its financial support.

REFERENCES

1. H. Matthies and G. Strang, The solution of nonlinear finite element equations. *Int. J. Numer. Meth. Engng* **14**, 1613–1626 (1979).
2. C. Pétiau and C. Cornuault, Algorithmes efficaces pour les calculs en post-flambement. *Proc. of 6th Symp. on Computing Meths in Applied Science and Engineering*, Versailles, France (1983).
3. M. Fafard, G. Dhatt and D. Beaulieu, Calcul automatique des configurations pré et post-flambement en calcul non linéaire des structures. Report GCT-87-06, Civil Engineering Department, Laval University, Québec, Canada (1987).
4. J. L. Batoz and G. Dhatt, Incremental displacement algorithms for non-linear problems. *Int. J. Numer. Meth. Engng* **14**, 1262–1266 (1979).
5. G. A. Wempner, Discrete approximations related to nonlinear theories of solids. *Int. J. Solids Struct.* **7**, 1581–1599 (1971).
6. E. Riks, An incremental approach to the solution of snapping and buckling problems. *Int. J. Solids Struct.* **15**, 529–551 (1979).
7. M. A. Crisfield, A fast incremental/iterative solution procedure that handles snap-through. *Comput. Struct.* **13**, 55–62 (1981).
8. E. Ramm, Strategies for tracing the non-linear response near limit points. In *Nonlinear Finite Element Analysis in Structural Mechanics*, pp. 68–89. Springer, New York (1981).
9. J. Padovan and R. Moscarello, Locally bound constrained Newton–Raphson solution algorithms. *Comput. Struct.* **23**, 181–197 (1986).
10. E. Akoussah, D. Beaulieu and G. Dhatt, Analyse non linéaire des structures à parois minces par éléments finis et son application aux bâtiments industriels. Report GCI-87-07, Civil Engineering Department, Laval University, Québec, Canada (1987).
11. H. Stegmüller, L. Hafner, E. Ramm and J. M. Sattler, Theoretische Grundlagen zum FE-programm system NISA 80. Mitteilung Nr. 1, Institut für Baustatik der Universität Stuttgart, Germany (1983).
12. V. Roman and A. E. Elwi, Postbuckling behavior of thin steel cylinders under transverse shear. Structural Engineering Report No 146, Department of Civil Engineering, University of Alberta, Edmonton, Canada (1987).
13. B. Massicotte, A. E. Elwi and J. G. MacGregor, Tension-stiffening model for planar reinforced concrete members. *J. Struct. Engng, ASCE* **116**, 3039–3058 (1990).
14. B. Massicotte, J. G. MacGregor and A. E. Elwi, Behavior of concrete panels subjected to axial and lateral loads. *J. Struct. Engng, ASCE* **116**, 2324–2343 (1990).